Structural studies of a polysaccharide from *Vibrio parahaemolyticus* strain AN-16000[†]

Carolina Fontana[a,b], Mona Zaccheus[a], Andrej Weintraub[c], Mohammad Ansaruzzaman[d], Göran Widmalm[a*]

[a] Department of Organic Chemistry, Arrhenius Laboratory, Stockholm University, S-106 91 Stockholm, Sweden

[b] Current address: Departamento de Química del Litoral, Centro Universitario de Paysandú (ref. académica Facultad de Química), Universidad de la República, Paysandú, C.P. 60000, Uruguay.

[c] Karolinska Institute, Department of Laboratory Medicine, Division of Clinical Microbiology, Karolinska University Hospital, S-141 86 Stockholm, Sweden

[d] International Centre for Diarrhoeal Disease Research, Dhaka 1000, Bangladesh

[†] Presented at the 4th Baltic meeting on Microbial Carbohydrates, Hyytiälä Forestry Field Station, Finland, September 19-22, 2010, poster no. 15.

Abstract

The structure of a polysaccharide from *Vibrio parahaemolyticus* strain AN-16000 has been investigated. The sugar and absolute configuration analysis revealed D-Glc, D-GalN, D-QuiN and L-FucN as major components. The PS was subjected to dephosphorylation with aqueous 40% HF to obtain an oligosaccharide that was analyzed by ^{1}H and ^{13}C NMR spectroscopy. The HR-MS spectrum of the oligosaccharide revealed a pentasaccharide composed of two Glc residues, one QuiNAc and one FucNAc, as well as a glycerol moiety. The structure of the PS was determined using ^{1}H, ^{13}C, ^{15}N and ^{31}P NMR spectroscopy; inter-residue correlations were identified by ^{1}H,^{13}C-heteronuclear multiple-bond correlation, ^{1}H,^{1}H-NOESY and ^{1}H,^{31}P-hetero-TOCSY experiments. The PS has the following teichoic acid-like structure:

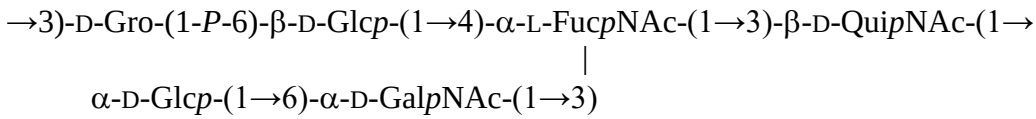

Keywords: *Vibrio parahemolyticus*, NMR, dephosphorylation, glycerol-3-phosphate

* Corresponding author. Tel.: +46 8 163 742. E-mail address: goran.widmalm@su.se

1. Introduction

Vibrio parahaemolyticus are curved rod-shaped, gram-negative, halophilic and highly motile bacteria that usually inhabit estuarine and coastal waters. Higher concentrations of these microorganisms are observed during summer time, when the salt content and temperature of the water favor the growth of the bacteria. These pathogens can cause gastroenteritis in humans, which is associated with the consumption of raw or poorly cooked seafood. They can also cause skin infections, although less frequently, when an open wound is exposed to contaminated warm seawater, or produce septicemia in immunocompromised patients.[1–4]

V. parahaemolyticus associated gastroenteritis was first reported in Japan in the 1950s, and since the 1970s many outbreaks have been observed in other coastal areas worldwide, extending from Asia to the American continent.[3] In order to facilitate epidemiological studies, the strains of *V. parahaemolyticus* are classified in different serotypes based on the serological properties of their somatic (O) and capsular (K) antigens; the flagellar (H) antigen is not employed in the serotyping scheme, since it is considered specific for each *Vibrio* species (*i.e.* all the strains of *V. parahaemolyticus* share the same H antigen).[5,6] In this regard, thirteen O-groups and seventy K-groups have been described to date, giving rise to a large number of possible serotypes.[3,7–10] In particular, the O3:K6, O4:K68, O1:K25, O1:K26, and O1:KUT serotypes have reached pandemic status since 1995 and are collectively known as the "pandemic group".[3,11–13] The clinical isolate used in this study (strain AN-16000) was obtained in 1998 at the International Centre for Diarrhoeal Disease Research (Bangladesh) and belongs to the pandemic O1:KUT serovar.[12,14] Herein we report the structural elucidation of a polysaccharide (PS) isolated from the aforementioned AN-16000 strain, using mainly NMR spectroscopy. Unlike the other *V. parahaemolyticus* PS structures that have been already reported in the literature (such as those obtained from the R-type LPS[15] of strains belonging to the O2, O6 and O12 serogroups, and the O-untypable KX-V212 strain[16–20]) this polysaccharide is composed of oligosaccharide repeating units.

2. Results

V. parahaemolyticus AN-16000 was grown in a Luria-Bertani medium and a polysaccharide (PS) was isolated from the water phase of a phenol-water extraction procedure.[21] Sugar analysis of the PS showed 2-amino-2,6-dideoxyglucose (quinovosamine), 2-amino-2,6-dideoxygalactose (fucosamine), glucose and 2-amino-2-deoxygalactose (galactosamine) as major components, in a ratio

1.4:0.5:1.8:1.2, respectively. GLC analysis of the acetylated (+)-2-butyl glycosides obtained from the PS revealed that QuiN, Glc and GalN have the D-configuration, whereas FucN has the L-configuration.

The ^{1}H and ^{13}C NMR spectra of the PS showed five resonances that could be attributed to anomeric atoms (Fig. 1), indicating that the PS consists of pentasaccharide repeating units. Three resonances were observed in the ^{1}H spectrum between 1.95 – 2.02 ppm (singlets, 3H each), indicating that the aminosugars are *N*-acetylated. This is consistent with the resonances observed in the ^{13}C spectrum between 22.98 – 23.17 ppm (3 methyl carbons) and 174.24 – 174.72 ppm (3 carbonyl carbons). Two resonances attributed to the H6 and C6 resonances of 6-deoxy-sugars were observed in both the ^{1}H (1.32 and 1.33 ppm) and ^{13}C (16.19 and 17.61 ppm) spectra, consistent with the presence of FucNAc and QuiNAc. The splitting of the ^{13}C resonances at 64.98, 67.19, 70.30 and 75.85 ppm indicated the presence of phosphorous (2.8, 7.7, 5.1 and 6.9 Hz, respectively), which was confirmed by the presence of a single phosphorous resonance at 1.35 ppm in the ^{31}P NMR spectrum of the PS.

2.1. Structure of the oligosaccharide obtained by dephosphorylation of the PS

The PS was dephosphorylated with aqueous 40% hydrofluoric acid and the resulting mixture was purified by size exclusion chromatography to yield an oligosaccharide, which was analyzed by mass spectrometry (MS). The HR-MS spectrum, in the positive mode, of the underivatized oligosaccharide showed, inter alia, a peak at *m/z* 1016.3879 corresponding to a compound of molecular formula $C_{39}H_{67}N_3O_{26}Na$ (calculated value 1016.3905) that was attributed to the pseudomolecular ion $[M+Na]^+$, whereas the spectrum recorded in the negative mode showed a strong peak at *m/z* 1028.3656 corresponding to a compound of molecular formula $C_{39}H_{67}N_3O_{26}Cl$ (calculated value 1028.3707) that was attributed to the pseudomolecular ion $[M+Cl]^-$. This information, together with the aforementioned sugar analysis, revealed that the oligosaccharide is composed of one QuiNAc, one FucNAc, two Glc and one GalNAc, in addition to one residue that may correspond to a glycerol moiety.

The multiplicity-edited $^{1}H,^{13}C$-HSQC NMR spectrum of the oligosaccharide showed five resonances in the anomeric region (δ_H/δ_C = 5.073/98.30, 4.998/98.36, 4.934/97.38, 4.643/103.82 and 4.426/102.44 ppm), corresponding to hexopyranosyl residues. The sugar residues were denoted **A** – **E** in order of decreasing chemical shifts of their anomeric protons (Fig. 2, bottom). The assignments of the ^{1}H resonances within each monosaccharide spin system were carried out using $^{1}H,^{1}H$-TOCSY spectra recorded with different mixing times (20, 40, 60 and 100 ms). The correlation patterns

observed in these spectra revealed that residues **C**, **D** and **E** have the *gluco*-configuration (i.e., all the protons up to H6 could be traced from the anomeric resonances in the spectrum with the longest mixing time) and residues **A** and **B** have the *galacto*-configuration (only protons up to H4 could be traced from the anomeric resonances, due to their small $^{3}J_{H4,H5}$ coupling). Correlations from H4 to H5 in residues **A** and **B** were obtained using a ^{1}H,^{1}H-NOESY spectrum. The assignment of the ^{13}C resonances were carried out using multiplicity-edited ^{1}H,^{13}C-HSQC (Fig. 2) and ^{1}H,^{13}C-H2BC spectra. The H6/C6 resonances of residues **B** and **E** are present at 1.329/16.11 and 1.335/17.47 ppm, respectively (Fig. 2, top), indicating that these are 6-deoxy-hexoses. The cross-peaks of the three hydroxymethyl groups in the hexose residues (**A**, **C** and **D**), and two in the glycerol moiety (**F**), are shown in red color in Fig. 2, middle. The C2 resonance of residues **A**, **B** and **E** are observed between 50.05 and 56.61 ppm indicating that these are nitrogen-bearing carbons. The carbonyl resonances from the *N*-acetyl groups (174.19, 174.66 and 174.78 ppm) were correlated to their respective methyl resonances (δ_H/δ_C 1.940/22.93, 1.954/22.74 and 2.022/23.05, respectively, cf. Fig. 2, top) using an aliased ^{1}H,^{13}C-HMBC spectrum; the carbonyl resonances at 174.78 and 174.19 ppm were also correlated to the proton resonances at 4.149 (H2 in residue **A**) and 4.362 ppm (H2 in residue **B**), respectively. Furthermore, in the ^{1}H,^{1}H-NOESY spectrum correlations were observed from the methyl groups at 1.940, 1.954 and 2.022 ppm to H2 in residues **B**, **E** and **A**, respectively. Residues **A**, **B** and **E** are then D-Gal*p*NAc, L-FucpNAc and D-QuipNAc, respectively, whereas **C** and **D** are D-Glc*p* residues. The configuration of the anomeric centers were determined by analysis of $^{3}J_{H1,H2}$ (obtained from a 1D ^{1}H spectrum) and $^{1}J_{C1,H1}$ couplings (obtained from a coupled ^{1}H,^{13}C-HSQC spectrum). Residues **A**, **B** and **C** are α-linked since they have $^{3}J_{H1,H2}$ = 3.4 – 4.1 Hz and $^{1}J_{C1,H1}$ = 170 – 173 Hz, whereas residues **D** and **E** are β-linked since they have $^{3}J_{H1,H2}$ = 7.9 – 8.6 Hz and $^{1}J_{C1,H1}$ = 160 – 163 Hz.[22] The ^{1}H and ^{13}C chemical shifts assignments of the oligosaccharide are compiled in Table 1, and they are compared to those of the corresponding monosaccharides.[23,24]

The substitution positions for the monosaccharide residues in the oligosaccharide were identified from ^{13}C glycosylation shifts.[23–25] Residue **A** is →6)-α-D-Gal*p*NAc-(1→ since $\Delta\delta_{C6}$ = 3.90 ppm, residue **B** is →3,4)-α-L-Fuc*p*NAc-(1→ since $\Delta\delta_{C3}$ = 1.83 ppm and $\Delta\delta_{C4}$ = 6.11 ppm and residue **E** is →3)-β-D-Qui*p*NAc-(1→ since $\Delta\delta_{C3}$ = 4.11 ppm. Residues **C** and **D** do not show any significant glycosylation shift for C2 – C6 and thus are α-D-Glc*p*-(1→ and β-D-Glc*p*-(1→ residues, respectively.

The sequence of the sugar residues in the oligosaccharide was determined using ^{1}H,^{1}H-NOESY and ^{1}H,^{13}C-HMBC experiments. Inter-residue ^{1}H,^{1}H-NOESY correlations were observed

from all the anomeric protons to the proton at the respective substitution positions (cf. Table 1). Consequently, the structure of the branched pentasaccharide-glycerol compound obtained by dephosphorylation of the PS of *V. parahaemolyticus* AN-16000 is: β-D-Glc*p*-(1→4)[α-D-Glc*p*-(1→6)-α-D-Gal*p*NAc-(1→3)]-α-L-Fuc*p*NAc-(1→3)-β-D-Qui*p*NAc-(1→1)-Gro. The three-bond heteronuclear correlations observed in the ^{1}H,^{13}C-HMBC spectrum from the anomeric carbons to the protons at the substitution positions, as well as from the anomeric protons to the glycosyloxylated carbons, are also consistent with the aforementioned structure (cf. Table 1).

2.2. Structure of the polysaccharide

The diffusion-filtered ^{1}H NMR of the PS from *V. parahaemolyticus* AN-16000, in which the anomeric resonance of each monosaccharide residue is annotated, is shown in Fig. 1 (*top*). The next step in the structural analysis employed a PANSY NMR experiment[26] in which a ^{1}H-decoupled ^{13}C spectrum (Fig. 1, *middle*) was acquired on a parallel receiver during the 120 ms mixing time of a ^{1}H,^{1}H-TOCSY experiment (Fig. 1, *bottom*). The ^{13}C NMR spectrum showed, inter alia, five anomeric carbon resonances in the region between 97.98 – 104.09 ppm. In the ^{1}H,^{1}H-TOCSY spectrum, the correlation patterns of the spin-systems originating from the anomeric protons indicate that residues **A** and **B** have the *galacto*-configuration whereas residues **C**, **D** and **E** have the *gluco*-configuration. The ^{13}C resonances of the sugar residues were assigned using a multiplicity-edited ^{1}H,^{13}C-HSQC spectrum (Fig. 3), as well as a ^{1}H,^{13}C-H2BC spectrum. The upfield chemical shifts of the C2 signals in residues **A**, **B** and **E** (49.92, 49.87 and 56.59 ppm, respectively) indicate that these are nitrogen-bearing carbons (Fig. 3, *middle*). Residues **B** and **E** are 6-deoxy hexoses since δ_H/δ_C are 1.32/16.19 and 1.33/ 17.61, respectively. The $^{1}J_{C1,H1}$ couplings were obtained from a ^{1}H,^{13}C-CT-CE-HSQC spectrum (in green color in Fig. 3, *bottom*), which confirmed that residues **A**, **B** and **C** are α-linked ($^{1}J_{C1,H1}$ = 168 – 176 Hz) and residues **D** and **E** are β-linked ($^{1}J_{C1,H1}$ = 162 Hz). Consequently, residues **A**, **B** and **E** are Gal*p*NAc, Fuc*p*NAc and Qui*p*NAc, respectively, whereas residues **C** and **D** are both Glc*p*. In addition to the aforementioned monosaccharide residues, resonances attributed to a glycerol residue (**F**) were also identified.

A band-selective constant-time ^{1}H,^{13}C-HMBC NMR experiment, performed with a ^{13}C selective pulse centered at the carbonyl resonance frequencies, was used for the assignment of the *N*-acetyl groups via $^{2}J_{C,H}$ and $^{3}J_{C,H}$ couplings. The carbonyl ^{13}C resonances at 174.68, 174.24 and 174.72 ppm showed correlations to their respective methyl protons (Fig. 4a), as well as to δ_H 4.16 (H2 in **A**),

δ_H 4.39 (H2 in **B**) and δ_H 3.85 (H2 in **E**), respectively (Fig. 4b). The amide proton chemical shifts were determined from a ^{1}H NMR spectrum recorded in a 95:5 H_2O:D_2O mixture (Fig. 4c), and correlated to the resonances of the respective nitrogen atoms using a ^{1}H,^{15}N-HSQC spectrum (Fig. 4d). The amide proton resonances were assigned to their corresponding sugar residues using ^{1}H,^{1}H-TOCSY (Fig. 4e-f) and ^{1}H,^{1}H-NOESY (Fig. 4g-h) experiments. The ^{1}H, ^{13}C and ^{15}N chemical shifts assignments of the repeating unit of the PS are compiled in Table 2, and the ^{1}H and ^{13}C chemical shifts are compared to those of the corresponding monosaccharides

The substitution positions in the sugar residues were identified from the ^{13}C NMR glycosylation shifts.[23–25] Analogously to what was described for the oligosaccharide material, residue **A** is →6)-α-D-Gal*p*NAc-(1→ since $\Delta\delta_{C6}$ = 4.66 ppm, residue **B** is →3,4)-α-L-Fuc*p*NAc-(1→ since $\Delta\delta_{C3}$ = 2.17 ppm and $\Delta\delta_{C4}$ = 6.53 ppm, residue **E** is →3)-β-D-Qui*p*NAc-(1→ since $\Delta\delta_{C3}$ = 4.37 ppm and residues **C** is α-D-Glc*p*-(1→ since it does not show any significant glycosylation shift for C2 – C6. However, in this case residue **D** is –6)-β-D-Glc*p*-(1→ since $\Delta\delta_{C6}$ = 3.14 ppm.

The splitting of some ^{13}C resonances resonances of glycerol (C1 and C2), and residue **D** (C5 and C6), due to $^nJ_{P,C}$ couplings, revealed the presence of a phosphorous atom linked to these residues. The ^{31}P NMR spectrum showed a single resonance at 1.35 ppm, consistent with the presence of a phosphodiester group.[27–29] The exact location of the phosphorous atom was identified using ^{1}H-^{31}P correlations from 2D heteronuclear experiments. The ^{1}H,^{31}P-HMBC spectra showed strong correlations from the phosphorous resonance to H6a/H6b in residue **D** and H1a/H1b in the glycerol residue (**F**) (cf. Table 3), whereas the ^{1}H,^{31}P-hetero-TOCSY spectra allowed the identification of additional protons in the spin system of both **D** and **F** residues (Fig. 5, *top*). Furthermore, the C1 resonance (phosphorylated position) of the glycerol moiety (residue **F**) in the PS is found 3.96 ppm downfield with respect to that of the C3 resonance of the glycerol moiety in the oligosaccharide (non-substituted position due to dephosphorylation). Consequently, residue **F** is →3)-Gro-(1-*P*–, and it is connected to C6 of residue **D** via a phosphodiester linkage.

The sequence of the sugar residues in the PS was determined using ^{1}H,^{13}C-HMBC and ^{1}H,^{1}H-NOESY experiments. Three-bond heteronuclear correlations were observed from the anomeric proton of each monosaccharide residue to their respective glycosyloxylated carbons (Fig. 5, *bottom*), as well as correlations from anomeric carbons to the protons at the respective substitution positions (Table 3). Consequently, the structure of the repeating unit of the PS isolated from *V. parahaemolyticus* AN-16000 is shown in SNFG-notation[30] and standard nomenclature in Fig. 6 (top and bottom,

respectively). The inter-residue ^{1}H,^{1}H-NOESY correlations from the anomeric protons of residues **A** – **E** to the protons in the respective substitution positions are also consistent with the proposed structure (Table 3). Additional inter-residue correlations were also observed from the anomeric protons of the α-linked residues **A** and **B** to the methyl and in particular the amide protons of the *N*-acetyl group of the 3-substituted residues **B** and **E**, respectively (Table 3 and Fig. 4h). Based on biosynthetic considerations, the absolute configuration of the glycerol moiety is tentatively assigned to D-glycerol 1-phosphate (D-Gro-1-*P*).[31–33]

3. Discussion

The structure of the PS of *V. parahaemolyticus* strain AN-16000 is remarkably similar to that of the O-antigen PS of *Proteus vulgaris* O12,[34] with the only difference being the presence of a β-D-Qui*p*NAc residue (in the former) instead of a β-D-Glc*p*NAc (in the latter). This structural difference is also shared by the O-PS of *Escherichia coli* O29, *Shigella dysenteriae* type 11, *Hafnia alvei* strain 1220, *Yersinia kristensenii* O25,35 and *Y. kristensenii* O12,25,[35–40] since all of them have a 3-substituted β-D-Glc*p*NAc residue in their backbone (highlighted in red color in Fig. 7) instead of the aforementioned 6-deoxy-aminosugar. Furthermore, in the case of *H. alvei* and *Y. kristensenii* strains the β-D-Glc*p*NAc residue is substituted at the O6 (*H. alvei*) or O4 (*Y. kristensenii*) position either with a α-D-Glc*p* (*H. alvei* and *Y. kristensenii* O25,35) or a β-D-Glc*p*NAc (*Y. kristensenii* O12,25) residue (highlighted in green color in Fig. 7). In the case of *E. coli* O29, *S. dysenteriae* type 11, *H. alvei* strain 1220 and *Y. kristensenii* O25,35, the monosaccharide that extends from the O3 position of α-L-Fuc*p*NAc is a 6-substituted α-D-galactopyranosyl residue (shown in blue color in Fig. 7) instead of a α-D-Gal*p*NAc residue (found in the PS of both *V. parahaemolyticus* AN-16000 and *Y. kristensenii* O12,25). Finally, the O-PS of the O25,35 and O12,25 serogroups of *Y. kristensenii* contain a 2-substituted D-glycerol 1-phosphate residue, instead of a →3)-Gro-(1-*P*– moiety (highlighted in magenta color in Fig. 7).

According to information available in the Bacterial Carbohydrate Structural Database (BCSDB)[41] L-Gro-1-*P* has not been found yet as a component of any gram-negative PS (i.e. even though some O-antigens have been reported to contain L-Gro-1-*P* in the past, such as in the case of *Shigella dysenteriae* type 11 and *Providencia alcalifaciens* O8,[36,42] new reports indicate that the configuration has been shown erroneously in the original articles).[37,43] In contrast, the occurrence of D-Gro-1-*P* has been reported and confirmed in many gram-negative PSs using either a methodology

developed by Rundlöf and Widmalm.[44] (in the case of the O-antigen PSs of *P. mirabilis* O54a,b and O40, *P. vulgaris* O54a,c and O12, *E. coli* O29 and O28ac, *H. alvei* strain 1207, *A. caviae* strain ATCC 15468, *C. werkmanii* O14, and the core oligosaccharide of *C. psychrerythraea* strain 34H)[27,34,35,45–50] or genetic information (in the case of the O-antigen PS of *E. coli* O42 and the CPS of *C. jejuni* HS:1).[51,52]

The absolute configuration of the glycerol moiety in the PS of *V. parahaemolyticus* AN-16000 has not been determined in this study, but it is assumed to be D-glycerol 1-phosphate (D-Gro-1-*P*) based on the observations described above and biosynthetic considerations. The biosynthesis of D-Gro-1-*P* can take place via two different mechanisms: *i)* through the reduction of dihydroxyacetone-phosphate (DHAP) with an NAD(P)H-dependent *sn*-glycerol 3-phosphate dehydrogenase (G3PDH) or *ii)* through the phosphorylation of glycerol with an ATP-dependent glycerol kinase.[31–33] D-Gro-1-*P* is used as a precursor in the biosynthesis of PS from both gram-negative and gram-positive bacteria. One should note that even though the teoichoic acids of gram-positive bacteria are composed of L-Gro-1-*P* moieties, the precursor used for their biosynthesis (phosphatidylglycerol) is actually obtained from D-Gro-1-*P*, and the glycerolphosphate subunits are then added through the action of a lipoteichoic acid synthase (LtaS) enzyme.[53–56] However, free L-Gro-1-*P* can be produced in archaea through the reduction of dihydroxyacetone-phosphate (DHAP) with an NAD(P)H-dependent *sn*-glycerol 1-phosphate dehydrogenase (G1PDH).[33,57,58] Furthermore, even though the existence of a bacterial G1PDH was reported by Guldan *et al.* in 2008, till date it has never been detected in any gram-negative species.[59]

4. Experimental

4.1. Bacterial strain, conditions of growth and isolation of the polysaccharide

The strain AN-16000 of *V. parahaemolyticus* (O1:KUT) was obtained as previously reported.[60] The bacteria were grown essentially as described,[61] and the PS was extracted by the hot phenol-water procedure followed by extensive dialysis against water and subsequent lyophilization.

Dephosphorylation of the PS

The PS (20 mg) was treated with 2 mL of aq. NH_4OH (12.5%) for 14 h at 37 °C. The solvent was evaporated with a stream of dry air and the crude material was treated with 1 mL of aqueous 40% HF at 4 °C for 3 days. At 0 °C evaporation of the solvent was carried out with a stream of dry air, H_2O was added and the solution neutralized with 1 M NH_4OH (aq.). The solution was then concentrated to

0.5 mL and centrifuged; the supernatant was purified by size exclusion chromatography on a HiLoad™ 16/60 Superdex™ 30 column (GE Healthcare), eluted with 1% 1-butanol in water at a flow rate of 1 mL·min^{-1} using an ÄKTA™ purifier system. RI and UV detection at 214 nm were used to monitor elution. The fully dephosphorylated oligosaccharide (~0.5 mg) was identified in a fraction eluting at a retention volume of 80 – 85 mL, and used for NMR analysis. The oligosaccharide material used for mass spectrometry analysis was obtained in a similar manner, but the dephosphorylation procedure was carried out directly on the native PS material.

4.2. Mass spectrometry

The electrospray ionization high-resolution mass spectrum (ESI-HRMS) was recorded in positive mode using a MicrOTOF-Q™ mass spectrometer (Bruker Daltonics).

4.3. Sugar analysis and absolute configuration determination

The PS (0.6 mg) was hydrolyzed with 4 M HCl at 100 °C for 30 min, and the released monosaccharides were reduced with $NaBH_4$ and acetylated. The mixture of alditol acetates was analyzed by gas-liquid chromatography (GLC). The absolute configuration of the sugar components was determined by GLC analysis of their acetylated (+)-2-butyl glycosides derivatives essentially as described using also racemic 2-butanol.[62]

4.4. GLC analyses

The alditol acetates and the acetylated 2-butyl glycosides but those from one sugar were separated using a temperature program on a PerkinElmer Elite-5 column with hydrogen as the carrier gas (25 psi) using a temperature program of 150 °C for 2 min, 3 °C min^{-1} up to 220 °C and then 10 min at 220 °C. The injector temperature and detector temperature were set to 220 and 250 °C, respectively. The butyl glycoside derivatives of galactosamine were separated on a PerkinElmer Elite-225 column with hydrogen as the carrier gas (25 psi) using a temperature program of 130 °C for 5 °C min^{-1} up to 150 °C, 7 °C min^{-1} up to 220 °C and then 20 min at 220 °C. The injector temperature and detector temperature were set to 140 and 250 °C, respectively. The columns were fitted to a PerkinElmer Clarus 400 Gas Chromatograph equipped with a flame ionization detector. Retention times of the derivatives were compared with those of authentic reference compounds. The O-antigen

polysaccharides of *E. coli* O26[63] and *P. penneri*[64] were used as references for fucosamine and quinovosamine, respectively.

4.5. NMR Spectroscopy

The NMR experiments were carried out on a Bruker AVANCE III 700 MHz spectrometer equipped with a 5 mm TCI Z-Gradient CryoProbe ($^{1}H/^{13}C/^{15}N$) and dual receivers, unless otherwise specified. The ^{1}H and ^{13}C chemical shifts assignments of the oligosaccharide material (~0.5 mg) were carried out in D_2O solution (0.18 mL, in a 3 mm NMR tube) at 298 K. The ^{1}H, ^{13}C and ^{31}P chemical shift assignments of the PS (4 mg) were performed in D_2O (0.55 mL) at 335 K. Amide protons and ^{15}N chemical shifts assignments were obtained from a solution of the PS (5.8 mg) in a 95:5 mixture H_2O:D_2O (0.55 mL). Chemical shifts are reported in ppm using external sodium 3-trimethylsilyl-(2,2,3,3-$^{2}H_4$)-propanoate (TSP, δ_H 0.00), 1,4-dioxane in D_2O (δ_C 67.40) or 2% H_3PO_4 in D_2O (δ_P 0.00) as references. The ^{15}N NMR chemical shifts were indirectly referenced as described by Wishart *et al.*[65] using $^{15}N/^{1}H$ = 0.101329. The chemical shifts were compared to those of the corresponding monosaccharides.[23,24]

The diffusion-filtered ^{1}H NMR spectrum of the PS was obtained on a Bruker AVANCE III 600 MHz spectrometer equipped with 5-mm inverse Z-gradient (55.7 $G \cdot cm^{-1}$) TXI ($^{1}H/^{13}C/^{31}P$) probes, using a pulsed-field-gradient (PFG) stimulated echo experiment with bipolar gradient pulses and one spoil gradient.[66] A diffusion time (Δ) of 0.10 s and diffusion encoded gradient pulses ($\delta/2$) of 1.8 ms were used; the PFG strength was 40% of the maximum. An exponential weighting function using a line-broadening factor of 0.3 Hz was applied prior to Fourier transformation of the FID.

The ^{1}H chemical shifts assignments were accomplished using $^{1}H,^{1}H$-TOCSY experiments[67] with mixing times between 10 and 100 ms, employing an MLEV-17 spin-lock of 10 kHz. The PANSY experiment,[26] in which a ^{1}H-decoupled ^{13}C spectrum was recorded on a parallel receiver during the 120 ms DIPSI spin-lock of a 2D $^{1}H,^{1}H$-TOCSY experiment, was obtained at the higher magnetic field.

The multiplicity-edited $^{1}H,^{13}C$-HSQC experiments[68] were recorded using smoothed CHIRP adiabatic pulses[69,70] for ^{13}C inversion and composite smoothed CHIRP for ^{13}C refocusing. The H2BC experiments[71] were recorded with constant time delays for J_{HH} evolution of 22 or 33 ms. The $^{1}J_{C1,H1}$ coupling constants of the PS and oligosaccharide materials were obtained using a $^{1}H,^{13}C$-CT-CE-HSQC experiment[72] and a ^{13}C-coupled multiplicity-edited $^{1}H,^{13}C$-HSQC experiment, respectively

The $^{1}H,^{1}H$-NOESY experiment[73] was recorded using a mixing time of 100 ms. The $^{1}H,^{13}C$-HMBC experiments[74] were carried out using two- or three-fold low-pass *J*-filters (J_{max} = 175 Hz and

J_{min} = 145 – 150 Hz) and a delay for evolution of long-range couplings of 62.5 ms. The band-selective constant-time $^{1}H,^{13}C$-HMBC experiment[75] was recorded with a 50 ms delay for the evolution of long-range couplings and a selective ^{13}C excitation pulse (Q3 Gaussian cascade) of 2.5 ms centered at the carbonyl resonance frequencies.

The $^{1}H,^{31}P$-hetero-TOCSY spectra[76] were recorded on a Bruker AVANCE II 500 MHz spectrometer equipped with 5 mm BBO Z-Gradient probe with mixing times of 20 and 60 ms; a DIPSI2 mixing sequence set at 5 kHz on both channels was employed. The $^{1}H,^{31}P$-HMBC spectra[77,78] were recorded on a Bruker AVANCE III 600 MHz spectrometer equipped with 5-mm inverse Z-gradient TXI ($^{1}H/^{13}C/^{31}P$) probe using delays for evolution of long-range couplings of 100, 10 and 2.5 ms.

The chemical shifts assignments of amide protons and nitrogens were obtained from spectra recorded on a Bruker AVANCE III 600 MHz spectrometer equipped with 5-mm inverse Z-gradient TXI ($^{1}H/^{13}C/^{15}N$) probe. The chemical shifts of the amide protons were extracted from a 1D ^{1}H spectrum recorded with water suppression by the excitation sculpting technique;[79] a selective square-shaped pulse of 2 ms was employed. A $^{1}H,^{15}N$-HSQC experiment[68] was used for assignment of the amide nitrogen resonances. $^{1}H,^{1}H$-TOCSY (mixing time 20, 40, 60 and 100 ms) and $^{1}H,^{1}H$-NOESY (mixing time 100 ms) experiments with water suppression by excitation sculpting were employed to correlate the amide protons to the corresponding sugar residues.

Acknowledgements

This work was supported by grants from the Swedish Research Council and the Knut and Alice Wallenberg Foundation. The research that has led to these results has received funding from the European Commission's Seventh Framework Programme FP7/2007-2013 under grant agreement no. 215536.

References

1. Wang, R.; Zhong, Y.; Gu, X.; Yuan, J.; Saeed, A. F.; Wang, S. *Front. Microbiol.* **2015**, *6*, 144.
2. Letchumanan, V.; Chan, K.-G.; Lee, L.-H. *Front. Microbiol.* **2014**, *5*, 705.
3. Nair, G. B.; Ramamurthy, T.; Bhattacharya, S. K.; Dutta, B.; Takeda, Y.; Sack, D. A. *Clin. Microbiol. Rev.* **2007**, *20*, 39–48.
4. Broberg, C. A.; Calder, T. J.; Orth, K. *Microbes Infect.* **2011**, *13*, 992–1001.

5. Tassin, M. G.; Siebeling, R. J.; Roberts, N. C.; Larson, A. D. *J. Clin. Microbiol.* **1983**, *18*, 400–407.

6. Sakazaki, R. Bacteriology of Vibrio and Related Organisms. In *Cholera*; Barua, D., Greenough, W. B., Eds.; Plenum Medical Book Company: New York, 1992; pp 37–55.

7. Terada, Y.; Yokoo, Y. *Japanase J. Bacteriol.* **1972**, *27*, 35–41.

8. Ishibashi, M.; Kinoshita, Y.; Miyano, K.; Niihara, T.; Kunita, N.; Takeda, Y.; Miwatani, T. *Japanase J. Bacteriol.* **1979**, *34*, 395–401.

9. Hisatsune, K.; Iguchi, T.; Haishima, Y.; Tamura, N.; Kondo, S. *Microbiol. Immunol.* **1993**, *37*, 143–147.

10. Lewandowski, C. M.; Co-investigator, N.; Lewandowski, C. M. *Japanase J. Bacteriol.* **2000**, *55*, 539–541.

11. Chowdhury, N. R.; Chakraborty, S.; Ramamurthy, T.; Nishibuchi, M.; Yamasaki, S.; Takeda, Y.; Nair, G. B. *Emerg. Infect. Dis.* **2000**, *6*, 631–636.

12. Matsumoto, C.; Okuda, J.; Ishibashi, M.; Iwanaga, M.; Garg, P.; Rammamurthy, T.; Wong, H.-C.; Depaola, A.; Kim, Y. B.; Albert, M. J.; Nishibuchi, M. *J. Clin. Microbiol.* **2000**, *38*, 578–585.

13. Boyd, E. F.; Cohen, A.; Naughton, L. M.; Ussery, D. W.; Binnewies, T. T.; Stine, O. C.; Parent, M. A. *BMC Microbiol.* **2008**, *8*, 110.

14. Okura, M.; Osawa, R.; Iguchi, A.; Arakawa, E.; Terajima, J.; Watanabe, H. *J. Clin. Microbiol.* **2003**, *41*, 4676–4682.

15. Iguchi, T.; Kondo, S.; Hisatsune, K. *FEMS Microbiol. Lett.* **1995**, *130*, 287–292.

16. Kondo, S.; Watabe, T.; Haishima, Y.; Hisatsune, K. *Carbohydr. Res.* **1993**, *245*, 353–359.

17. Isshiki, Y.; Kondo, S. *Microbiol. Immunol.* **2011**, *55*, 539–551.

18. Kondo, S.; Zähringer, U.; Seydel, U.; Sinnwell, V.; Hisatsune, K.; Rietschel, E. T. *Eur. J. Biochem.* **1991**, *200*, 689–698.

19. Hashii, N.; Isshiki, Y.; Iguchi, T.; Kondo, S. *Carbohydr. Res.* **2003**, *338*, 2711–2719.

20. Hashii, N.; Isshiki, Y.; Iguchi, T.; Kondo, S.; Hisatsune, K. *Carbohydr. Res.* **2003**, *338*, 1063–1071.

21. Westphal O, J. K. *Methods Carbohydr. Chem.* **1965**, *5*, 83–91.

22. Bundle, D. R.; Lemieux, R. U. *Methods Carbohydr. Chem.* **1976**, *7*, 79–86.

23. Jansson, P.-E.; Kenne, L.; Widmalm, G. *Carbohydr. Res.* **1989**, *188*, 169–191.

24. Lundborg, M.; Widmalm, G. *Anal. Chem.* **2011**, *83*, 10–13.

25. Söderman, P.; Jansson, P.-E.; Widmalm, G. *J. Chem. Soc. Perkin Trans. 2* **1998**, 639–648.

26. Kupče, Ē.; Freeman, R.; John, B. K. *J. Am. Chem. Soc.* **2006**, *128*, 9606–9607.

27. Rundlöf, T.; Weintraub, A.; Widmalm, G. *Carbohydr. Res.* **1996**, *291*, 127–139.

28. Linnerborg, M.; Weintraub, A.; Widmalm, G. *Carbohydr. Res.* **1999**, *320*, 200–208.

29. Landersjö, C.; Weintraub, A.; Widmalm, G. *Eur. J. Biochem.* **2001**, *268*, 2239–2245.

30. Varki, A.; Cummings, R. D.; Aebi, M.; Packer, N. H.; Seeberger, P. H.; Esko, J. D.; Stanley, P.; Hart, G.; Darvill, A.; Kinoshita, T.; Prestegard, J. H.; Schnaar, R. L.; Freeze, H. H.; Marth, J. D.; Bertozzi, C. R.; Etzler, M. E.; Frank, M.; Vliegenthart, J. F. G.; Lütteke, T.; Perez, S.; Bolton, E.; Rudd, P.; Paulson, J.; Kanehisa, M.; Toukach, P.; Aoki-Kinoshita, K. F.; Dell, A.; Narimatsu, H.; York, W.; Taniguchi, N.; Kornfeld, S. *Glycobiology* **2015**, *25*, 1323–1324.

31. Fuchs, G. Biosynthesis of Building Blocks. In *Biology of the Prokaryotes*; Lengeler, J. W., Drews, G., Schlegel, H. G., Eds.; Georg Thieme Verlag: Stuttgart, 1999; pp 110–160.

32. LeBlanc, D. J. *Prokaryotes* **2006**, *4*, 175–204.

33. Koga, Y.; Morii, H. *Microbiol. Mol. Biol. Rev.* **2007**, *71*, 97–120.

34. Perepelov, A. V.; Torzewska, A.; Shashkov, A. S.; Senchenkova, S. N.; Rozalski, A.; Knirel, Y. A. *Eur. J. Biochem.* **2000**, *267*, 788–793.

35. Perepelov, A. V.; Wang, Q.; Senchenkova, S. N.; Shevelev, S. D.; Zhao, G.; Shashkov, A. S.; Feng, L.; Knirel, Y. A.; Wang, L. *Carbohydr. Res.* **2006**, *341*, 2176–2180.

36. Liu, B.; Knirel, Y. A.; Feng, L.; Perepelov, A. V.; Senchenkova, S. N.; Wang, Q.; Reeves, P. R.; Wang, L. *FEMS Microbiol. Rev.* **2008**, *32*, 627–653.

37. Liu, B.; Knirel, Y. a; Feng, L.; Perepelov, A. V; Senchenkova, S. N.; Wang, Q.; Reeves, P. R.; Wang, L. *FEMS Microbiol. Rev.* **2010**, *34*, 606.

38. Dabrowski, U.; Dabrowski, J.; Katzenellenbogen, E.; Bogulska, M.; Romanowska, E. *Carbohydr. Res.* **1996**, *287*, 91–100.

39. Gorshkova, R. P.; Isakov, V. V.; Nazarenko, E. L.; Ovodov, Y. S.; Guryanova, S. V.; Dmitriev, B. A. *Carbohydr. Res. Res.* **1993**, *241*, 201–208.

40. L'vov, V. L.; Gur'yanova, S. V.; Rodionov, A. V.; Gorshkova, R. P. *Carbohydr. Res.* **1992**, *228*, 415–422.

41. Toukach, P. V.; Egorova, K. S. *Nucleic Acids* **2015**, *44*, D1229–D1236.

42. Toukach, F. V.; Kocharova, N. A.; Maszewska, A.; Shashkov, A. S.; Knirel, Y. A.; Rozalski, A. *Carbohydr. Res.* **2008**, *343*, 2706–2711.

43. Knirel, Y. A. Structure of O-antigens. In *Bacterial Lipopolysaccharides. Structure, Chemical Synthesis, Biogenesis and Interaction with Host Cells*; Knirel, Y. A., Valvano, M. A., Eds.; Springer: Vienna, 2011; pp 41–115.

44. Rundlöf, T.; Widmalm, G. *Anal. Biochem.* **1996**, *243*, 228–233.

45. Kondakova, A. N.; Fudala, R.; Senchenkova, S. N.; Shashkov, A. S.; Knirel, Y. A.; Kaca, W. *Carbohydr. Res.* **2005**, *340*, 1612–1617.

46. Kołodziejska, K.; Perepelov, A. V.; Zabłotni, A.; Drzewiecka, D.; Senchenkova, S. N.; Zych, K.; Shashkov, A. S.; Knirel, Y. A.; Sidorczyk, Z. *FEMS Immunol. Med. Microbiol.* **2006**, *47*, 267–274.

47. Jachymek, W.; Czaja, J.; Niedziela, T.; Lugowski, C.; Kenne, L. *FEBS J.* **1999**, *266*, 53–61.

48. Wang, Z.; Liu, X.; Li, J.; Altman, E. *Carbohydr. Res.* **2008**, *343*, 483–488.

49. Katzenellenbogen, E.; Kocharova, N. A.; Korzeniowska-kowal, A.; Bogulska, M.; Rybka, J.; Gamian, A.; Kachala, V. V.; Shashkov, A. S.; Knirel, Y. A. *FEMS Immunol. Med. Microbiol.* **2008**, *54*, 255–262.

50. Carillo, S.; Pieretti, G.; Lindner, B.; Parrilli, E.; Filomena, S.; Tutino, M. L.; Lanzetta, R.; Parrilli, M.; Corsaro, M. M. *European J. Org. Chem.* **2013**, 3771–3779.

51. Fontana, C.; Weintraub, A.; Widmalm, G. *Carbohydr. Res.* **2014**, *403*, 174–181.

52. Karlyshev, A. V; Champion, O. L.; Churcher, C.; Brisson, J.; Jarrell, H. C.; Gilbert, M.; Brochu, D.; Michael, F. S.; Li, J.; Wakarchuk, W. W.; Goodhead, I.; Sanders, M.; Stevens, K.; White, B.; Parkhill, J.; Wren, B. W.; Szymanski, C. M. *Mol. Microbiol.* **2005**, *55*, 90–103.

53. Percy, M. G.; Gründling, A. *Annu. Rev. Microbiol.* **2014**, *68*, 81–100.

54. Schneewind, O.; Missiakas, D. *J. Bacteriol.* **2014**, *196*, 1133–1142.

55. Grundling, A.; Schneewind, O. *Proc. Natl. Acad. Sci. U. S. A.* **2007**, *104*, 8478–8483.

56. Lu, D.; Wormann, M. E.; Zhang, X.; Schneewind, O.; Grundling, A.; Freemont, P. S. *Proc. Natl. Acad. Sci. U. S. A.* **2009**, *106*, 1584–1589.

57. Koga, Y.; Kyuragi, T.; Nishihara, M.; Sone, N. *J. Mol. Evol.* **1998**, *46*, 54–63.

58. Carbone, V.; Schofield, L. R.; Zhang, Y.; Sang, C.; Dey, D.; Hannus, I. M.; Martin, W. F.; Sutherland-Smith, A. J.; Ronimus, R. S. *J. Biol. Chem.* **2015**, *290*, 21690–21704.

59. Guldan, H.; Sterner, R.; Babinger, P. *Biochemistry* **2008**, *47*, 7376–7384.

60. Bhuiyan, N. A.; Ansaruzzaman, M.; Kamruzzaman, M.; Alam, K.; Chowdhury, N. R.; Nishibuchi, M.; Faruque, S. M.; Sack, D. A.; Takeda, Y.; Nair, G. B. *J. Clin. Microbiol.* **2002**, *40*, 284–286.

61. Svensson, M. V.; Weintraub, A.; Widmalm, G. *Carbohydr. Res.* **2011**, *346*, 449–453.

62. Leontein, K.; Lönngren, J. *Methods Carbohydr. Chem.* **1993**, *9*, 87–89.

63. Manca, M. C.; Weintraub, A.; Widmalm, G. *Carbohydr. Res.* **1996**, *281*, 155–160.

64. Shashkov, A. S.; Arbatsky, N. P.; Widmalm, G.; Knirel, Y. A.; Zych, K.; Sidorczyk, Z. *Eur. J. Biochem.* **1998**, *253*, 730–733.

65. Wishart, D. S.; Bigam, C. G.; Yao, J.; Abildgaard, F.; Dyson, H. J.; Oldfield, E.; Markley, J. L.; Sykes, B. D. *J. Biomol. NMR* **1995**, *6*, 135–140.

66. Wu, D.; Chen, A.; Johnson, C. S. *J. Magn. Reson. Ser. A* **1995**, *115*, 260–264.

67. Bax, A.; Davis, D. G. *J. Magn. Reson.* **1985**, *65*, 355–360.

68. Schleucher, J.; Schwendinger, M.; Sattler, M.; Schmidt, P.; Schedletzky, O.; Glaser, S. J.; Sørensen, O. W.; Griesinger, C. *J. Biomol. NMR* **1994**, *4*, 301–306.

69. Kupče, Ē. *Methods Enzymol.* **2002**, *338*, 82–111.

70. Tannús, A.; Garwood, M. *NMR Biomed.* **1997**, *10*, 423–434.

71. Nyberg, N. T.; Duus, J. Ø.; Sørensen, O. W. *J. Am. Chem. Soc.* **2005**, *127*, 6154–6155.

72. Tian, F.; Al-Hashimi, H. M.; Craighead, J. L.; Prestegard, J. H. *J. Am. Chem. Soc.* **2001**, *123*,

485–492.

73. Kumar, A.; Ernst, R. R.; Wüthrich, K. *Biochem. Biophys. Res. Commun.* **1980**, *95*, 1–6.
74. Cicero, D. O.; Barbato, G.; Bazzo, R. *J. Magn. Reson.* **2001**, *148*, 209–213.
75. Claridge, T. D. W.; Pérez-Victoria, I. *Org. Biomol. Chem.* **2003**, *1*, 3632–3634.
76. Kellogg, G. W.; Szewczak, A. A.; Moore, P. B. *J. Am. Chem. Soc.* **1992**, *114*, 2727–2728.
77. Bax, A.; Summers, M. F. *J. Am. Chem. Soc.* **1986**, *108*, 2093–2094.
78. Zartler, E. R.; Martin, G. E. *J. Biomol. NMR* **2011**, *51*, 357–367.
79. Hwang, T.-L.; Shaka, A. J. *J. Magn. Reson. Ser. A* **1995**, *112*, 275–279.

Figure legends

Figure 1. Diffusion-filtered ^{1}H NMR spectrum of the PS from *V. parahaemolyticus* AN-16000 (*top*). Spectra resulting from a PANSY NMR experiment that utilizes dual receivers: selected region of the ^{1}H,^{1}H-TOCSY spectrum (τ_m = 120 ms) showing correlations from anomeric protons (*bottom*), and ^{13}C experiment with proton decoupling acquired in parallel during the spin-lock of the 2D experiment (*middle*). Note that the ^{1}H,^{1}H-TOCSY correlation between H1 and H6 of residue **E** is not shown, since the corresponding cross-peak lies outside the plotted region.

Figure 2. Selected regions of the multiplicity-edited ^{1}H,^{13}C-HSQC NMR spectrum of the pentasaccharide-glycerol obtained by dephosphorylation of the PS from *Vibrio parahaemolyticus* AN-16000 showing the anomeric region (**a**), the region for ring atoms and hydroxymethyl groups (in which the cross-peaks from the latter appear in red) (**b**) and the region for the methyl groups from 6-deoxy sugars and *N*-acetyl groups (**c**). Resonances from anomeric and substitution positions, as well as nitrogen-bearing carbons, are annotated.

Figure 3. a) Overlay of the anomeric region of the multiplicity-edited ^{1}H,^{13}C-HSQC and ^{1}H,^{13}C-CT-CE-HSQC NMR spectra of the PS from *V. parahaemolyticus* AN-16000 (black and green colored cross peaks, respectively). Selected regions of the multiplicity-edited ^{1}H,^{13}C-HSQC spectrum showing **b**) the region for the ring atoms and hydroxymethyl groups (in which the cross-peaks from the latter appear in red color) and **c**) the region for the methyl groups from 6-deoxy sugars and *N*-acetyl groups. Resonances from anomeric and substitution positions, as well as nitrogen-bearing carbons, are annotated. Note that the low intensity cross peaks originating from C1 of glycerol cannot be seen at this plot level.

Figure 4. a-b) Regions of the ^{1}H,^{13}C-BS-CT-HMBC NMR spectrum of the PS from *V. parahaemolyticus* AN-16000 recorded with enhanced resolution over the carbonyl region. **c**) The amide protons region of the ^{1}H NMR spectrum. **d**) The ^{1}H,^{15}N-HSQC spectrum showing correlations from the amide protons to the respective nitrogen atoms. Selected region of the: **e-f**) ^{1}H,^{1}H-TOCSY and **g-h**) ^{1}H,^{1}H-NOESY spectra (in both cases the mixing time was 100 ms) showing correlations from the amide protons. The spectra of panels **c-h** were recorded in a H_2O:D_2O mixture (95:5).

Figure 5. The ^{1}H,^{31}P-hetero-TOCSY NMR spectrum (mixing time 60 ms) of the PS from *V. parahaemolyticus* AN-16000 with pertinent annotations (*top*) and selected region of the ^{1}H,^{13}C-HMBC spectrum showing correlations from anomeric protons (*bottom*).

Figure 6. Structure of the repeating unit of the PS from *V. parahaemolyticus* AN-16000 in SNFG-notation (*top*) and standard nomenclature (*bottom*).

Figure 7. Comparison of the structures of the PS from *V. parahaemolyticus* AN-16000 and the O-antigen PS from *P. vulgaris* O12, *E. coli* O29/*S. dysenteriae* type 11, *H. alvei* strain 1220, *Yersinia kristensenii* O25,35 and O12,25 using standard nomenclature. The structural differences with respect to *V. parahaemolyticus* AN-16000 are highlighted in red, blue, green and magenta colors.